Structural and Magnetic Properties of Nanogranular $BaTiO_3$-$CoFe_2O_4$ Thin Films Deposited by Laser Ablation on Si/Pt Substrates

José Barbosa[1], Bernardo Almeida[1], Jorge A. Mendes[1], Anabela G. Rolo[1], João P. Araújo[2], and João B. Sousa[2]

[1]Departamento de Física, Universidade do Minho, Campus de Gualtar, Braga, 4710-057 Braga, Portugal
[2]Dep. de Física and IFIMUP, Universidade do Porto, Rua Campo Alegre, 687, Porto, 4169-007 Porto, Portugal

ABSTRACT

Thin film nanogranular composites of cobalt ferrite ($CoFe_2O_4$) dispersed in a barium titanate ($BaTiO_3$) matrix were deposited by laser ablation with different cobalt ferrite concentrations (*x*). The films were polycrystalline and composed by a mixture of tetragonal-$BaTiO_3$ and $CoFe_2O_4$ with the cubic spinnel structure. A slight (111) barium titanate phase orientation and (311) $CoFe_2O_4$ phase orientation was observed. As the concentration of the cobalt ferrite increased, the grain size of the $BaTiO_3$ phase decreased, from 91nm to 30nm, up to 50% $CoFe_2O_4$ concentration, beyond which the $BaTiO_3$ grain size take values in the range 30-35nm. On the other hand the cobalt ferrite grain size did not show a clear trend with increasing cobalt ferrite concentration, fluctuating in the range 25nm to 30nm. The lattice parameter of the $CoFe_2O_4$ phase increased with increasing *x*. However, it was always smaller than the bulk value indicating that, in the films, the cobalt ferrite was under compressive stress that was progressively relaxed with increasing $CoFe_2O_4$ concentration. The magnetic measurements showed a decrease of coercive field with increasing *x*, which was attributed to the relaxation of the stress in the films and to the increase of particle agglomeration in bigger polycrystalline clusters with increasing cobalt ferrite concentration.

INTRODUCTION

Recently, nanostructured multiferroic composites formed by the combination of a piezoelectric ceramic and a magnetostrictive material, such as in the $BaTiO_3$-$CoFe_2O_4$ system, have been attracting much scientific and technological interest [1]. In these systems, the elastic interactions between the phases provides the coupling mechanism inducing a magnetoelectric behavior [1,3]. As a result, the properties and performance of these nanostructures depend critically on the phase morphology and internal stress distribution, which, in turn, are determined by the elastic phase/phase and phase/substrate interactions.

In order to address this problem thin film nanocomposites of cobalt ferrite ($CoFe_2O_4$) dispersed in a barium titanate ($BaTiO_3$) matrix were deposited with different cobalt ferrite concentrations, as well as pure barium titanate and cobalt ferrite films (end members).

$CoFe_2O_4$ has a cubic inverse spinnel structure [4] in which the octahedral B sites are occupied by eight Co^{2+} and eight Fe^{3+} cations, while the tetrahedral A sites are occupied by the

remaining eight Fe^{3+}. It presents a high magnetocrystalline anisotropy and magnetostriction [5], making it suitable for application in magnetoelectric composite thin films.

$BaTiO_3$ is a well studied ferroelectric perovskite [6]. At high temperatures $BaTiO_3$ is cubic, in which the large barium ions are surrounded by twelve nearest-neighbor oxygens and each titanium ion has six oxygen ions in octahedral coordination. At a temperature ~395 K $BaTiO_3$ transforms from a cubic to a tetragonal structure, which in turn changes to an orthorhombic phase at ~280 K and finally to a rhombohedral phase at ~193 K. The ambient temperature tetragonal phase is ferroelectric and the high temperature cubic phase is paraelectric.

EXPERIMENTAL

The nanogranular $BaTiO_3$ - $CoFe_2O_4$ thin films were prepared by pulsed laser ablation, on platinum covered Si(001) substrates. The depositions were done with a KrF excimer laser (wavelength λ = 248 nm), at a fluence of 1.5 J/cm^2 and 10 Hz repetition rate. The oxygen pressure during deposition was pO_2 = 1 mbar and the substrate temperature was 600ºC. The ablation targets were prepared by mixing $CoFe_2O_4$ and $BaTiO_3$ powders with cobalt ferrite weight concentrations x = 20%, 30%, 40%, 50%, 60% and 70%. They were then compressed and sintered at 1200ºC during 1 hour. The end members targets, barium titanate and cobalt ferrite, were also prepared in this way. The structural studies were performed by X-ray diffraction (XRD) and were carried out with a Philips PW-1710 diffractometer using Cu Kα radiation. The films surface was examined using a Leica Cambridge S360 scanning electron microscope (SEM), with 10 kV operating voltage. Energy dispersive X-ray analysis (EDX) was used in order to perform chemical studies. Raman characterization was done using a Jobin-Yvon T64000 spectrometer with an excitation wavelength at 514.5 nm, from an Ar laser. The magnetic properties were measured with a Quantum Design MPMS SQUID magnetometer. The X-ray diffraction spectra measured on the laser ablation targets showed that they were polycrystalline and composed by mixtures of tetragonal-$BaTiO_3$ and $CoFe_2O_4$ with the cubic spinnel structure.

DISCUSSION

Figure 1a) shows the X-ray diffraction spectra measured on the nanocomposite thin films with cobalt ferrite concentrations in the range 20% - 100%. Figure 1b) shows a SEM micrograph obtained on the sample deposited with 40% cobalt ferrite concentration. The films are polycrystalline and composed by a mixture of tetragonal-$BaTiO_3$ and $CoFe_2O_4$ with the cubic inverse spinnel structure. They present a granular surface, as observed by SEM, with a broad range of grain sizes. The bigger grains observed in the micrograph of figure 1b) have an average size of 647nm. The concentration of the elements composing the films, obtained from EDX measurements on different regions (and grains) of the micrographs, is uniform over the analyzed area. Inherent to the laser ablation technique is the appearance of small droplets (~ 1 - 5 μm) on the films surface. In our samples, the surface shows a low density of these droplets.

The grain sizes as measured from the X-ray diffraction peak widths for both phases ((112) for $BaTiO_3$ and (311) for $CoFe_2O_4$), were determined by using the Scherrer equation [7]. They are shown in figure 2a) for the different nanocomposite films. The grain sizes are in the range 20nm to 100nm. However, as the concentration of the cobalt ferrite increases, the grain

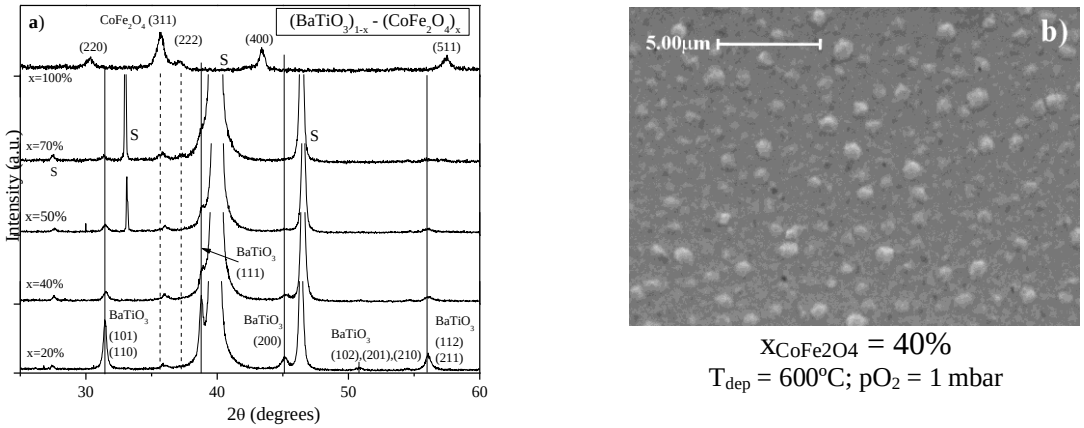

Figure 1. X-ray diffraction spectra of the samples deposited with $CoFe_2O_4$ concentrations in the range 20%-100% (a), and SEM micrograph obtained on the film with x = 40% (b). The vertical lines mark the peak position of the bulk $CoFe_2O_4$ cubic spinel phase (---), and the tetragonal-$BaTiO_3$ phase (—). The peaks marked with an S are from the substrate.

size of the $BaTiO_3$ phase decreases, from 91.5 nm to 30nm, up to 50% $CoFe_2O_4$ concentration beyond which the $BaTiO_3$ grain size fluctuates in the interval 30-35nm. On the other hand the cobalt ferrite grain size does not show a clear trend with increasing cobalt ferrite concentration, fluctuating in the range 25nm to 30nm. Since the average grain sizes of the phases composing the films are below 100nm and the SEM micrographs show the existence of a significant number of grains up to ~650 nm, this again indicates the presence of a broad distribution of grain sizes in the films.

Figure 2b) shows the relative intensity between the (111) peak and the (110),(101) peaks of the $BaTiO_3$ phase in the films, for different $CoFe_2O_4$ concentration. The (110),(101) peaks are the most intense ones in bulk tetragonal $BaTiO_3$. As the concentration of the cobalt ferrite increases, the relative intensity of the (111) $BaTiO_3$ peak increases, indicating a more oriented growth of this phase. The opposite occurs with the (311) peak from the $CoFe_2O_4$ phase. From

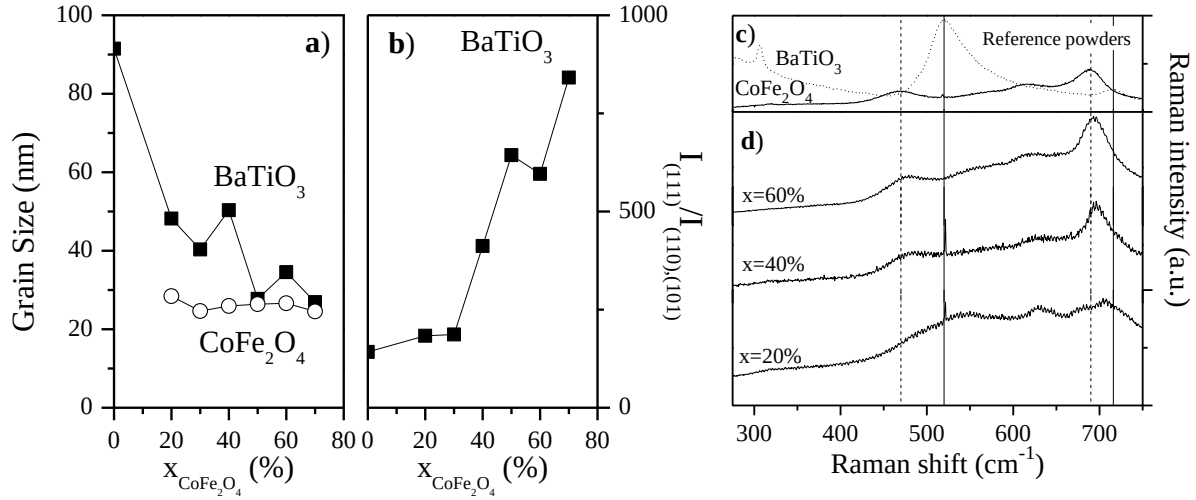

Figure 2. Grain sizes of the $BaTiO_3$ and $CoFe_2O_4$ phases (a) and relative intensity of the (111) peak (b), for different $CoFe_2O_4$ concentrations. Also shown are the Raman spectra measured on the c) bulk reference powders and d) nanocomposite films.

figure 1a), as *x* increases the (222) peak starts to appear, while the intensity of the (311) peak only slightly changes, indicating a progressive increase of the polycrystallinity of the $CoFe_2O_4$ phase in the films.

The lattice parameter of the cobalt ferrite phase was determined from the X-ray diffraction spectra measured on the nanocomposites. For $CoFe_2O_4$ it was obtained from the (311) peak position and varied from 8.26Å in the sample deposited with cobalt ferrite concentration x = 20%, to 8.35Å in the sample deposited with x = 70%. Comparing with the bulk $CoFe_2O_4$ lattice parameter (a = 8.3919Å), in the films the cobalt ferrite is under compressive stress that relaxes as its concentration progressively increases.

Figures 2c) and 2d) show the Raman spectra measured on individual tetragonal-$BaTiO_3$ and cubic-spinnel-$CoFe_2O_4$ bulk powders and on the thin film samples. The sharp peak appearing near 520 cm^{-1} is due to the characteristic plasma laser line from the Ar laser. Two main peaks are observed in the spectrum of the $CoFe_2O_4$ powder and of the nanocomposite films. They appear at 470 cm^{-1} and 690 cm^{-1} and their positions are represented by doted lines in figures 2c) and 2d). They were assigned to octahedral site (O-site) sublattice and tetrahedral site (T-site) sublattice vibration modes, respectively [8], and reflect the local lattice effects in the tetrahedral and octahedral sublattices. As the cobalt ferrite concentration is increased on the nanocomposite films these peaks become more pronounced indicating the increased contribution of the $CoFe_2O_4$ phase to the Raman spectra. Also, their peak positions are systematically above the corresponding bulk values. This blueshift of the $CoFe_2O_4$ modes results from the lattice strain as already observed on cobalt ferrite thin films with thicknesses near 50nm [9] and observed in our X-ray diffraction results. The peaks from $BaTiO_3$ are not so visible, but two slight bumps appear near 520 cm^{-1} and 716 cm^{-1}, corresponding to the $BaTiO_3$ transverse optical (TO) and longitudinal optical (LO) vibrations of the A_1 and E phonon modes [10].

Figure 3a) shows hysteresis loops measured on the nanocomposite films at the temperature T = 10 K. The loops were measured on the films plane and corrected by subtracting the diamagnetic contribution from the substrate. Figure 3b) shows the coercivity (at 10 K and 300 K) for the nanocomposite thin films, taken from the corresponding hysteresis loops. The magnetic measurements show an increase of the magnetic moment and a decrease of the coercive

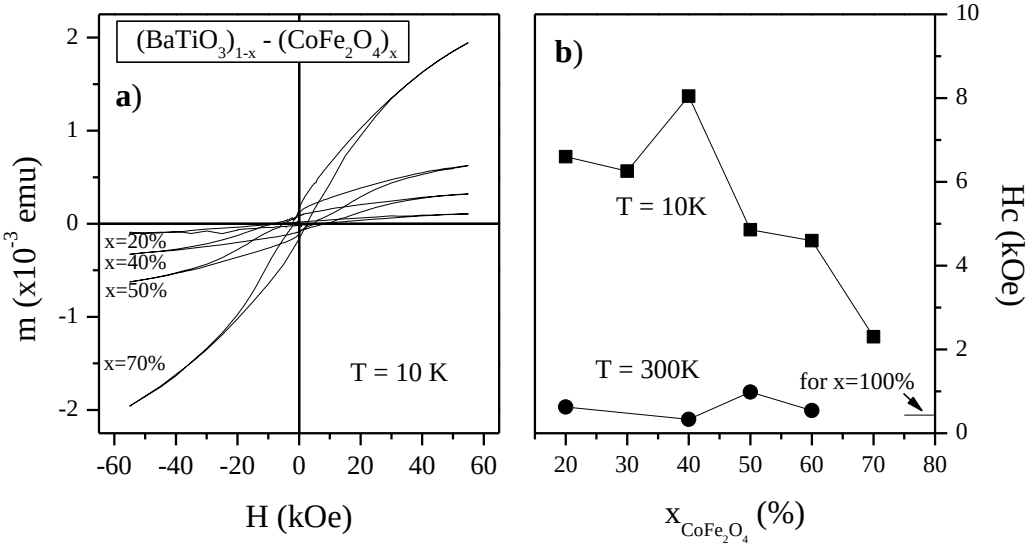

Figure 3: a) Magnetic hysteresis cycles of the nanocomposite $(BaTiO_3)_{1-x}$-$(CoFe_2O_4)_x$ films measured at T=10 K. b) Coercivity of the films at T=10K and T=300K. In b) the horizontal line marks the value obtained for x = 100%

field (Hc), from the low concentration region where the magnetic grains are more isolated, towards the higher $CoFe_2O_4$ content where the inter-particle magnetic coupling is higher.

At low temperatures, the thin films present a high coercivity (H_c) that decreases with increasing cobalt ferrite concentration. During deposition of the thin films, the cobalt ferrite phase nanograins are formed with a broad range of sizes, with average grain sizes between 25 nm and 30 nm as referred earlier. At lower $CoFe_2O_4$ concentration, the cobalt ferrite nanograins are more isolated. The coercivity of isolated Co-ferrite particles increases with increasing diameter and reaches maximum value for particles with diameters of about 40 nm [11,12]. Magnetization vector rotation is considered to be the mechanism responsible for the coercivity of small particles (smaller than 40 nm), where H_c is proportional to the magnetocrystalline anisotropy [4]. Additionally, the bigger particles (larger than 40 nm) divide into domains and the mechanism for coercivity depends on the stress in the films [4]. For low concentrations, the $CoFe_2O_4$ grains are more isolated weakening ferromagnetic interactions between them. Thus, the increased coercivity of smaller grains and the increased stress contributing to increased coercivity of larger grains add to a higher coercive field. As the cobalt ferrite concentration increases, the nanograins start to form larger clusters of less isolated nanoparticles. Also, the stress in the cobalt ferrite grains decreases. These effects combine to reduce the coercivity of the nanocomposite thin films with increasing $CoFe_2O_4$ concentrations. Also, the coercivity strongly decreases with increasing temperature, from 10 K to 300 K, due to the corresponding decrease of the magnetocrystalline anisotropy of $CoFe_2O_4$ [4,11]

CONCLUSIONS

Nanogranular composites of cobalt ferrite dispersed in a barium titanate matrix were deposited with different $CoFe_2O_4$ concentrations. Detailed structural and magnetic measurements were performed on the films. The barium titanate phase presented a tetragonal structure, while the cobalt ferrite had the cubic spinnel structure, and a broad distribution of grain sizes was present in the films. Additionally, the $CoFe_2O_4$ phase was under compressive stress that relaxed as its concentration increased. Thus, a decrease of the coercive field with increased $CoFe_2O_4$ concentration was observed, due to the relaxation of the stress in the films as well as to the increase of particle agglomeration in bigger polycrystalline clusters with increasing cobalt ferrite concentrations.

ACKNOWLEDGMENTS

This work has been financially supported by the Portuguese Foundation for Science and Technology (FCT), through the project POCI/CTM/60181/2004.

REFERENCES

1. W. Eerenstein, N.D. Mathur and J.F. Scott, Nature, **442**, 759 (2006)
2. M. Fiebig, J. Phys. D: Appl. Phys., **38**, R123 (2005)

3. H. Zheng, J. Wang, S.E. Lofland, Z. Ma, L. Mohaddes-Ardabili, T. Zhao, L. Salamanca-Riba, S.R. Shinde, S.B. Ogale, F. Bai, D. Viehland, Y. Jia, D.G. Schlom, M. Wuttig, A. Roytburd, R. Ramesh, Science, **303**, 661 (2004)
4. S. Chikazumi, "Physics of Ferromagnetism", Oxford University Press, New York, (1997)
5. M. Grigorova, H.J. Blythe, V. Blaskov, V. Rusanov, V. Petkov, V. Masheva, D. Nihtianova, L.M. Martinez, J.S.Muñoz, M. Mikhov, J. Magn. Magn. Mat. **183** 163 (1998)
6. Seung-Eek Park, S. Wada, L.E. Cross, and T.R. Shrout, J. Appl. Phys. **86**, 2746 (1999)
7. B.D. Cullity, "Elements of X-Ray Diffraction", Addison-Wesley, Reading MA, (1978)
8. T. Yu, Z.X. Shen, Y. Shi and J. Ding, J. Phys.: Condens. Matter, **14**, L613 (2002)
9. U.V. Venkateswaran, V.M. Naik and R. Naik, Phys. Rev. B, **58**, 14256 (1999)
10. Y.C. Wang, J. Ding, J.B. Yi, B.H. Liu, T. Yu, and Z.X. Shen, Appl. Phys. Lett., **84**, 2596 (2004)
11. C. N. Chinnasamy, B. Jeyadevan, K. Shinoda, K. Tohji, D. J. Djayaprawira M. Takahashi, R. Justin Joseyphus and A. Narayanasamy, Appl. Phys. Lett., **83**, 2862 (2003)
12. J.S. Jung, J.H. Lim, K.H. Choi, S.L. Oh, Y.R. Kim, and S.-H. Lee, D.A. Smith, K.L. Stokes, L.Malkinski, and C.J. O'Connor, J. Appl. Phys., **97**, 10F306 (2005)